Double-Lariat Caged Morpholino Oligonucleotides for Optical Gene Silencing

Sankha Pattanayak[1,5], Alexander Deiters[2] and James K. Chen[1,3,4]*

[1]Department of Chemical and Systems Biology, Stanford University School of Medicine, Stanford, California 94305, United States

[2]Department of Chemistry, University of Pittsburgh, Pittsburgh, Pennsylvania 15260, United States

[3]Department of Developmental Biology, Stanford University School of Medicine, Stanford, California 94305, United States

[4]Department of Chemistry, Stanford University, Stanford, California 94305, United States

[5]Current Address: Creyon Bio, Inc. San Diego, California 92121, United States

*Correspondence should be addressed to J.K.C. (jameschen@stanford.edu).

ABSTRACT

Caged morpholino oligonucleotides (cMOs) are synthetic tools that allow light-inducible gene silencing in live organisms. Previously reported cMOs have utilized hairpin, duplex, and cyclic structures, as well as caged nucleobases. While these optochemical technologies enable efficient optical gene silencing, they can have limited dynamic range. To address this issue, a new caging strategy was developed where the two MO termini are conjugated to an internal position through a self-immolative trifunctional linker, thereby generating a bicyclic cMO with a double lariat-like structure. The efficacy of this alternative cMO design has been demonstrated in zebrafish embryos and compared to the monocyclic constructs.

INTRODUCTION

Light-gated technologies have emerged as powerful research tools to decipher the molecular mechanisms that underlie complex biological systems.[1,2] Because specific tissues can be illuminated at precise timepoints, photoactivatable reagents are well-suited for inducing molecular perturbations in whole organisms with spatial and temporal control.[3,4] These technologies are particularly useful when applied in optically transparent model organisms that develop *ex utero* such as zebrafish,[5] sea urchins,[6] and ascidians.[7] Oligonucleotide-based reagents are especially versatile probes as they can be readily designed to specifically target any gene,[8,9] and phosphorodiamidate morpholino oligonucleotides (MOs) have been most commonly used to inhibit gene expression *in vivo*.[10,11,12] These synthetic DNA/RNA mimetics are composed of nucleobase-bearing morpholine rings connected with neutral phosphorodiamidate linkages (Figure 1A)[13] and constitute three out of the eleven FDA-approved oligonucleotide-based drugs in the last six years.[14] MOs are generally designed as 25-mer sequences that hybridize with their cognate RNAs to inhibit protein synthesis or alter splicing. These reagents typically are injected into early-stage embryos (e.g., one- to four-cell zebrafish zygotes) and become uniformly distributed throughout the animal.[15] As a result, standard MOs constitutively and ubiquitously silence their targeted genes, and in zebrafish embryos these reagents can be effective for up to five days.[16] To achieve spatiotemporal gene regulation, we and others have developed caged morpholino oligonucleotides (cMOs) that remain inactive until released by irradiation with light of specific wavelengths.

The first generation of photocaged morpholinos had a hairpin structure, in which a shorter inhibitory MO was used to restrict the 25-base MO from binding to its target mRNA (Figure 1B).[17,18] Multiple versions of the MO caging strategy were subsequently developed. For example, duplexes between the full-length MO and cleavable complementary oligonucleotides have been employed as cMOs (Figure 1B).[19,20] In another design, nucleobases were protected with photoremovable groups to prevent them from Watson-Crick base-pairing (Figure 1B).[21,22] However, each of these designs has certain drawbacks that limit their dynamic range. For instance, hairpin cMOs require careful tuning of the inhibitor binding energetics to minimize basal activity,[18] and the inhibitory MO can impart additional toxicity. The complementary oligonucleotides released by photoactivated duplex cMOs are also potentially toxic, and the nucleobase-caged reagents require photolysis of multiple caging groups, which can be challenging to achieve quantitatively. To address these issues, we and the Tang laboratory independently developed cyclic cMOs by tethering the oligonucleotide termini with a photocleavable linker (Figure 1B).[23,24] The curvature introduced by cyclization hinders cMO-RNA hybridization because oligonucleotide duplexes has limited conformational flexibility.[25]

The cyclic cMOs addressed several shortcomings of the previous generations.[23] This design does not require optimization of thermodynamic parameters, employs a single light-cleavable group, does not

liberate any oligonucleotide byproducts, and is readily synthesized from commercially available reagents. In addition, the modular linker chemistry of cyclic cMOs facilitates their design for other uncaging methods. For instance, while the first generation of cyclic cMOs was designed to be activated by ultraviolet light, we have subsequently reported cyclic cMOs that can be uncaged with blue light,[26,27] enzymes,[28] and small molecules[29]. Other versions of cyclic cMOs that contain ruthenium- or BHQ-based linkers have also been reported.[30,31] Cyclic cMOs have enabled optochemical control of multiple genes in zebrafish, including *no tail-a* (*tbxta), t-box gene* 16 (*tbx16*), *pancreas transcription factor 1 alpha* (*ptf1a*), *ets variant gene 2* (*etv2*), and *focal adhesion kinase* (*fak*).[32,23] Taking advantage of the spatiotemporal control afforded by cMOs, we have further demonstrated how these optochemical tools can be combined with photoactivatable lineage tracers, fluorescence-activated cell sorting, and transcriptome profiling to gain new insights into tissue-patterning mechanisms.[33,34]
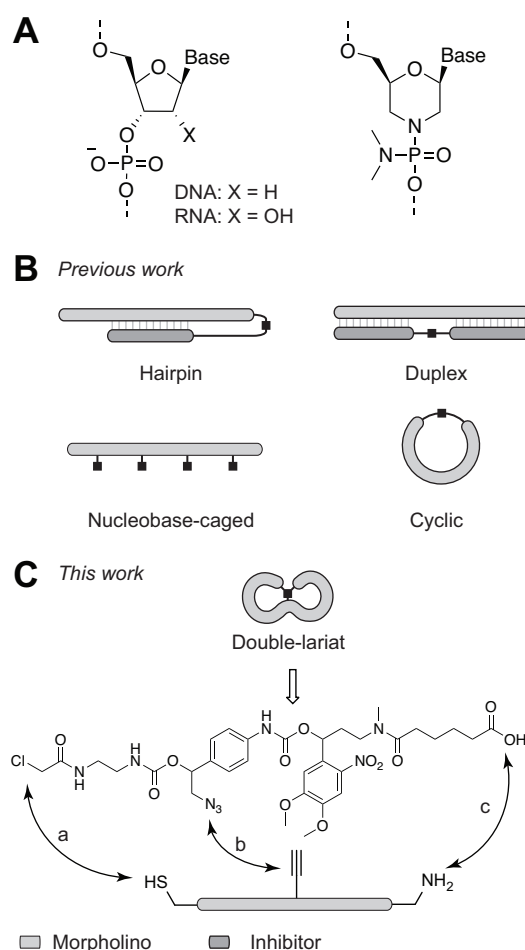

Figure 1. **Morpholino oligonucleotides and their caged derivatives.** A) Comparison of DNA/RNA and MO chemical structures. B) Current caged morpholino structural types. C) Double-lariat cMO structure and overview of the synthesis strategy. The double-lariat geometry can be achieved by three orthogonal bioconjugation reactions: a) thiol-halogen exchange, b) CuAAC click reaction, c) amide coupling.

Despite these successes, all current cMO structural types suffer from limited dynamic range. cMOs can inhibit their RNA targets to varying degrees prior to photoactivation, and finding a working dose that minimizes 'leak' and maximizes post-irradiation phenotypic penetrance can be challenging. The simultaneous application of two or more cMOs is even more likely to have significant basal activity. For example, while individual cyclic *tbxta* and *tbx16* cMOs work effectively, we were unable to combine these two reagents to study how these transcription factors act in combination to regulate mesoderm development in zebrafish embryos.[35] The combined 'leakiness' of these cyclic cMOs resulted in light-independent mesodermal defects in all tested concentrations. Overcoming these limitations is therefore critical to achieving the full potential of cMOs as tools for elucidating the mechanisms that regulate development, physiology, and disease.

To address these issues and build upon the cyclic cMO design, we report herein a new class of cMOs that tethers the MO termini to an internal position through a single photocleavable moiety, thereby generating a double-lariat structure. The photocleavable linker was designed to undergo light-dependent self-immolative cleavage, allowing release of the termini and MO linearization. We hypothesized that the smaller macrocycles and increased local curvature of these reagents would further limit RNA hybridization compared to standard cyclic cMOs.

RESULTS AND DISCUSSION

The cyclic cMO strategy validated that MO activity can be conformationally gated by macrocyclization.[23] In principle, a smaller macrocycle size would increase caging efficacy due to greater oligonucleotide curvature. To test this hypothesis, we previously synthesized non-cleavable cyclic *tbxta* MOs of varying size (21-, 23-, and 25-mers) and measured their melting temperatures (T_m's) with a complementary 25-base RNA.[23] While the smaller cyclic MOs exhibited reduced affinities towards the target RNA than the conventional 25-mer reagent, their uncaged products also were less potent in zebrafish embryos, as gauged by their ability to reduce Tbxta protein levels. Thus, it is essential to have 25-mer MOs to achieve efficient RNA targeting. We envisioned that a bicyclic caging strategy would preserve the required 25-mer length while forming smaller macrocycles, which could be achieved by tethering both MO termini to an internal nucleotide (Figure 1C).

While cyclic cMOs can be generated with bifunctional linkers, a trifunctional crosslinker is required for the double-lariat structure. Moreover, all three attachment points need to be released by a single photolytic reaction. To achieve both goals, we devised a novel self-immolative linker (Figure 1C) bearing a single photoremovable group upon photolysis which would trigger a spontaneous 1,6-elimination reaction to linearize the caged oligonucleotide (Figure 2). To generate the tandem-release core, we chose a photolabile 4,5-dimethoxy-2-nitrobenzyl (DMNB) group, which we used in our previous hairpin and cyclic cMO design.[18,23] In this case, the DMNB moiety was strategically linked

with a masked hydroxymethylaniline scaffold through a carbamate linkage, which was also employed in our nitroreductase- and small molecule-activatable cMOs.[28,29] The spontaneous 1,6-elimination reaction has been reported to be rapid ($t_{1/2} \sim 90$ s),[36] enabling cMO activation to occur within minutes after linker photocleavage. The methylenetriazole moiety in the benzylic position is further expected to accelerate the reaction.[37] We also selected three orthogonal reactive moieties for the self-immolative linker: a chloroacetamide, an azide-bearing hydroxymethylaniline, and a carboxylic acid-functionalized DMNB group. This trifunctional linker can undergo three sequential reactions with a linear MO bearing a thiol, internal alkyne, and amine, respectively (Figure 1C). After light-dependent linearization, the final MO would bear an aminophenyltriazole scar in the phosphorodiamidate linkage (Figure 2). MOs with substituted interlinkages have been shown to be tolerated for antisense applications.[38,39]
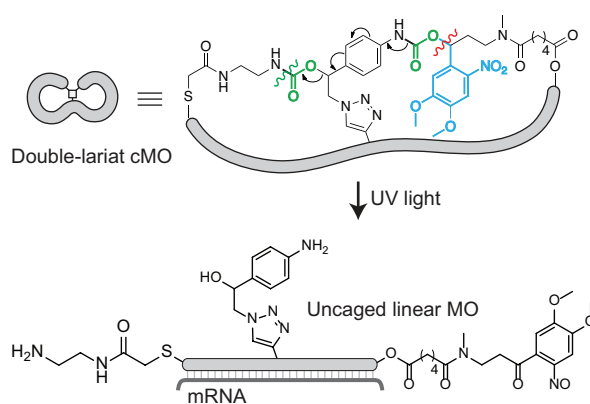

Figure 2. **Double-lariat cMO photoactivation.** Proposed uncaging mechanism and subsequent hybridization to the targeted mRNA. The photocleavage site (red), 1,6-elimination cascade (arrows), and CO_2 eliminations (green) have been shown.

According to our design, the self-immolative core in the linker (Figure 1C, and **10** in Scheme 1) includes a hydroxymethylaniline moiety with the aryl amine masked by a carbamate-linked DMNB photolabile group. Since most substituents at the benzylic position of the aniline are unstable due to the 1,6-elimination reaction, we planned to install the chloroacetamide moiety on the hydroxymethylaniline after building the self-immolative core. Accordingly, we first synthesized the TBS-protected azido hydroxymethylaniline **4** from commercially available 2-bromo-4'-nitroacetophenone **1** in six steps (Scheme 1). Sodium borohydride-mediated reduction of the α-bromoketone **1** and subsequent TBS protection provided protected α-bromo alcohol **2.** For the alcohol protection, the TBS group was chosen because it has been shown to be stable in other self-immolative systems.[40] Palladium-mediated hydrogenation of the nitro group of **2** yielded the aryl amine, which was subsequently protected with trifluoroacetic anhydride to obtain **3**. Substitution of this bromo compound with sodium azide afforded the corresponding azido derivative, which was then treated with methanolic ammonia to remove the trifluoroacetyl protection to afford the azide-bearing hydroxymethylaniline **4.**
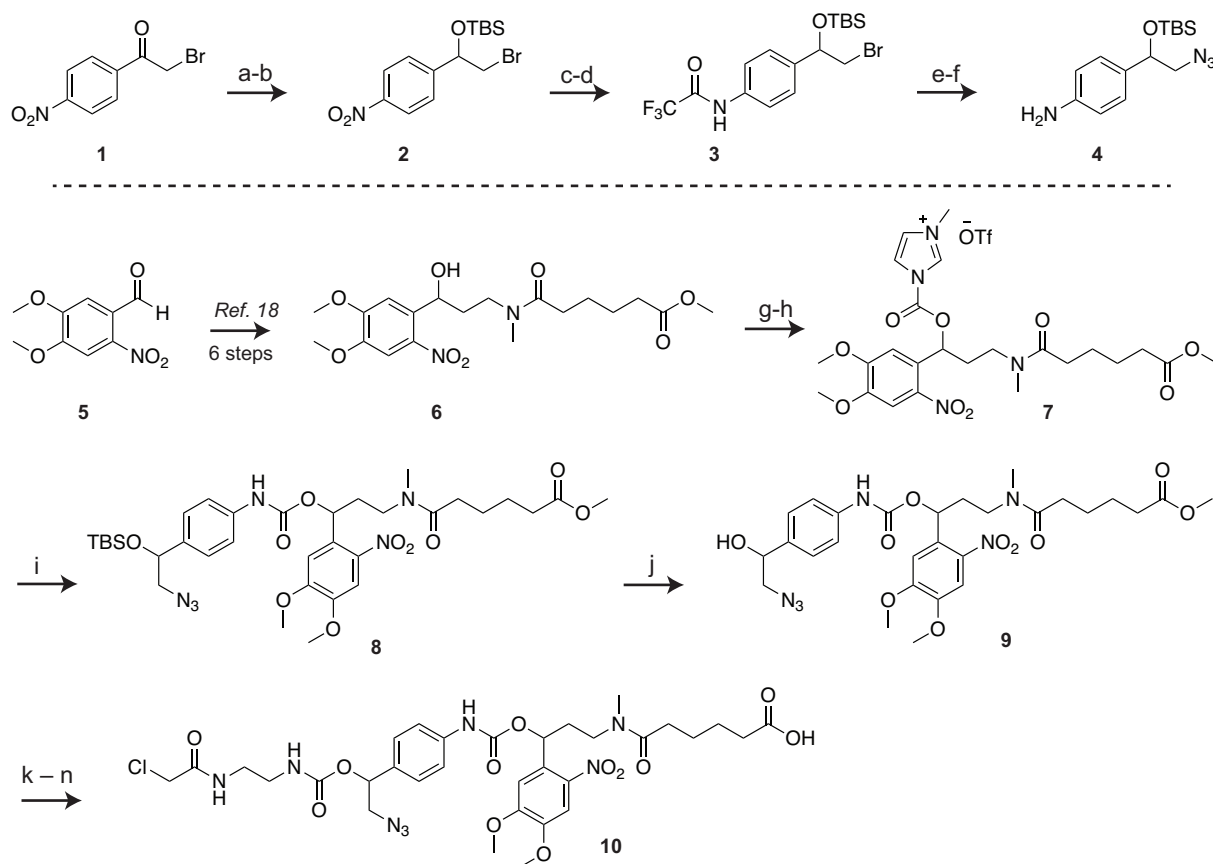
Scheme 1. **Synthesis of the self-immolative linker for the double-lariat cMO.** (a) NaBH$_4$, MeOH, 69%; (b) TBSCl, imidazole, DMF, 62%; (c) 5% Pd-C, H$_2$, THF, 87%; (d) (CF$_3$CO)$_2$O, DCM, 71%; (e) NaN$_3$, TBAI, DMF, 60 °C, 66%; (f) 7 M NH$_3$ in MeOH, 84%; (g) CDI, DCM; (h) MeOTf, DCM; (i) azido aniline **4**, DCM, 24% over three steps; (j) TBAF, THF, 80%; (k) CDI, DCM; (l) ethylenediamine, 91% over two steps; (m) chloroacetyl chloride, 48%; (n) LiOH, THF-H$_2$O, 75%.

To synthesize the rest of the trifunctional linker (Scheme 1), we prepared the DMNB-functionalized ester **6** from commercially available 4,5-dimethoxy-2-nitrobenzaldehyde **5**, following our earlier reports.[18] To form the self-immolative core, we then attempted to couple the secondary alcohol functionality of **6** with the aryl amine of azido hydroxymethylaniline **4** through a carbamate linkage. This coupling, however, posed a significant hurdle,[41] likely due to weak nucleophilicity of the aniline and steric hindrance of the secondary alcohol. Our attempts to form the carbamate linkage by activating the alcohol as an *N*-hydroxysuccinimide carbonate, chloroformate, or imidazolium carbamate were unreliable and only afforded a complex mixture of products. Activation of the aniline functionality of **4** by isocyanate formation with phosgene proceeded smoothly, but subsequent coupling with **6** was unsuccessful under several conditions. We finally successfully coupled these two components by activating the alcohol **6** as an *N*-methylimidazolium salt **7** (Rapoport's reagent type activation),[42] which to the best of our knowledge is the first example of hindered carbamate synthesis through *N*-methylimidazolium salt formation. The activated reagent **7** is not stable and had to be prepared *in situ* by a two-step sequence using carbonyl diimidazole (CDI) and methyl triflate immediately prior to use. Subsequent reaction of **7** with hydroxymethylaniline **4** afforded the product **8** containing the self-immolative core. To install the chloroacetamide sidechain, the TBS protection from **8** was first removed with fluoride treatment to obtain the alcohol **9**. The secondary alcohol **9** was

then activated with CDI and conjugated with ethylenediamine followed by capping with chloroacetyl chloride to yield the methyl ester intermediate. Subsequent hydrolysis of the methyl ester with lithium hydroxide provided the fully functionalized double-lariat linker **10**. We then confirmed that **10** can be cleaved by ultraviolet light by irradiating a dilute solution of the linker and monitored the resulting reaction by HPLC. We observed that the linker formed three products within 30 seconds of ultraviolet light exposure (see Supporting Information, Supplementary Figure S1).
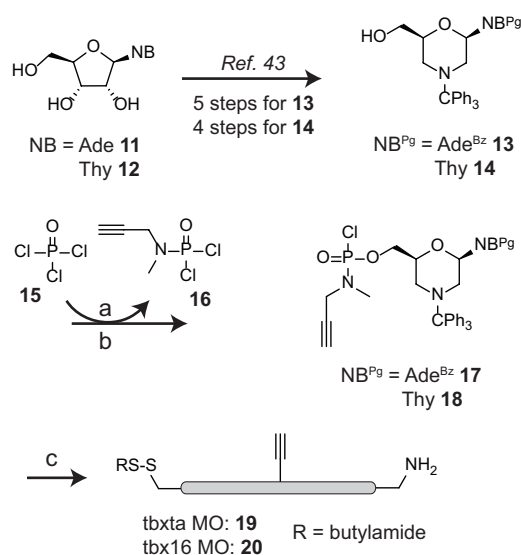

Scheme 2. **Synthesis of the trifunctionalized linear morpholinos.** (a) *N*-methylpropargylamine, triethylamine, DCM, 78%; (b) **19**, LiBr, DBU, DCM-acetonitrile, 46% for Ade; 51% for Thy (c) Incorporation into MO sequences by solid phase synthesis.

Unlike MOs with terminal disulfides and amines, internally modified MOs are not commercially available. To develop trifunctionalized MOs with an additional internal alkyne handle, we decided to incorporate the alkyne group into monomeric MO building blocks through an *N*-methylpropargylamine modification in place of a standard dimethylamine moiety (Scheme 2). Accordingly, we synthesized 5'-hydroxyl adenine and thymine morpholino monomers (**13** and **14**, respectively)[43,44] and developed the new propargylphosphoramidic dichloride reagent **16**. Activation of the hydroxyl monomers with DBU and lithium bromide afforded the corresponding chlorophosphoramidites **17** and **18**.[45] These monomers were then incorporated into the MOs during standard solid-phase synthesis. Since MOs are typically 25 nucleotides in length, we decided to include the alkyne moiety at the 12th or the 13th phosphoroamidate linkage, placing the alkyne handle in a central position. We chose to prepare two alkyne-functionalized MOs targeting zebrafish *tbxta* and *tbx16*, composed of the nucleotide sequences 5′-GACTTGAGGCAG**A**CATATTTCCGAT-3′ and 5′-CTCTGATAGCC**T**GCATTATTTAGC C-3′, respectively (alkyne-functionalized monomers denoted in bold). Having made the alkyne-functionalized MOs, we sought to confirm if the aminophenyltriazole scar in the final photocleavage product would interfere with gene inhibition in zebrafish embryos. We therefore prepared a model

photocleavage product by copper-mediated azide-alkyne cycloaddition (CuAAC) or 'click' reaction of *tbxta* MO **19** and the azide-bearing hydroxymethylaniline **4** (see Supporting Information, Supplementary Scheme S1). We then assessed its efficacy to inhibit the *tbxta* gene compared to a non-functionalized linear MO, as determined by the resulting notochord phenotypes. There was no appreciable difference between the model photocleavage product MO and the linear MO in their efficacy and toxicity (data not shown).

Having synthesized both the trifunctionalized linker and morpholinos, we next focused on developing an efficient synthetic protocol for double lariat formation. While our cyclic cMO version used amide coupling followed by a thiol-halogen exchange reaction to close the ring, we first decided to perform the CuAAC click reaction for the double-lariat cMO synthesis (Scheme 3). This would allow us to monitor the product formation with mass spectrometry, whereas conducting this cycloaddition reaction at a later stage would not lead to a change in molecular weight. In our optimized protocol (see Supporting Information), the alkyne-functionalized linear MOs (*tbxta* MO **19** or *tbx16* MO **20**) and the linker **10** were click-conjugated using copper iodide catalyst. Reducing agents such as sodium ascorbate were avoided because the disulfide end group was unstable in these conditions.[46] Formation of the cycloaddition product (*tbxta* MO **21** and *tbx16* MO **22**) was monitored by HPLC and mass spectrometry. Any unreacted linear morpholino was removed by further click reaction with azide-functionalized agarose beads.
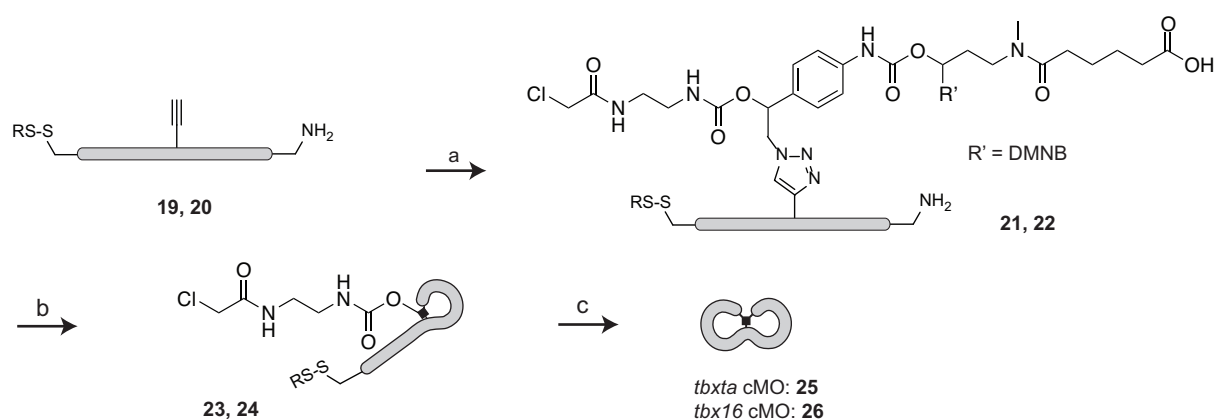
Scheme 3. **Synthesis of the double-lariat cMO.** (a) Linker **10**, CuI, tris(benzyltriazolylmethyl)amine (TBTA), DMSO, 0.5 M triethylammonium acetate (TEAA) buffer, 37 °C, 50 - 72%; (b) DMTMM, 100 mM MOPS - 1 M NaCl buffer, pH 7.5, 37 °C, 40 - 55%; (c) tris(2-carboxyethyl)phosphine hydrochloride (TCEP-HCl), 0.1 M Tris-HCl buffer, pH 7.5 then pH 8.5, 37 °C, 45 - 60%.

To generate the first lariat (*tbxta* MO **23** or *tbx16* MO **24**), we next performed the amide-coupling reaction by activating[47] the carboxylic acid end with a large excess of 4-(4,6-dimethoxy-1,3,5-triazin-2-yl)-4-methylmorpholinium chloride (DMTMM) (Scheme 3). Assuming all the free carboxylic acid was converted to activated ester, the reaction mixture was treated with ω-aminohexyl agarose resin to remove any linear morpholino. This method of removing the unreacted amine morpholino worked

better than NHS-functionalized resin treatment. The single-lariat oligonucleotides (*tbxta* MO **23** or *tbx16* MO **24**) were then isolated with a Nap-25 column. Although we were unable to find a suitable HPLC condition to separate the single lariat product from the linear conjugate (*tbxta* MO **21** or *tbx16* MO **22**), we could confirm the purity of the products **23** and **24** by mass spectrometry analysis. Finally, to prepare the second lariat, the terminal disulfide was reduced with brief treatment with tris(2-carboxyethyl)phosphine hydrochloride (TCEP•HCl). The reducing agent was removed by dialysis to avoid side reactions with the chloroacetamide group, and the resulting thiol reacted spontaneously with the chloroacetamide group by thiol-halogen exchange reaction to form the desired double-lariat cMO (*tbxta* MO **25** or *tbx16* MO **26**). Unlike our cyclic cMOs synthesis, treatment with TCEP•HCl solution provided cleaner reaction profile than resin-immobilized TCEP. The reaction mixture was then treated with maleimide-functionalized agarose beads to remove any unreacted single-lariat MO, and the final double-lariat cMO was purified with Nap-5 columns and confirmed by mass spectroscopy.

To test our new caging strategy *in vivo*, we evaluated the double-lariat *tbxta and tbx16* cMOs in zebrafish embryos. Tbxta, the zebrafish orthologue of mammalian Brachyury has an essential role in the differentiation of axial mesoderm progenitors into notochord cells.[48] Tbxta deficiency results in the loss of notochord and posterior mesoderm, as well as abnormal U-shaped somites due to the loss of notochord-derived signals.[49,50] We have previously found that a 1 ng/embryo (~115 fmol) dose of the linear *tbxta* MO recapitulates the *tbxta* mutant phenotype in zebrafish embryos.[17,18] Accordingly, we injected an equivalent amount of the double-lariat cMO into one-cell zebrafish zygotes and irradiated the embryos at 3.5 hours post-fertilization (hpf) with ultraviolet light (365 nm) for 15 seconds or cultured them in the dark. The embryos were then scored at 24 hpf using a morphology-based system that includes four mesodermal phenotypes.[18] To compare basal activities of the new double-lariat cMOs, we also assessed their efficacies side-by-side with a cyclic *tbxta* cMO in zebrafish embryos (Figure 3A). We found that *tbxta* double-lariat cMO was comparable to the cyclic reagent in terms of basal activity. Close to 85% of the embryos developed normally in both cases without any developmental defects when raised in the dark. However, we noticed that the double-lariat cMO exhibited lower activity recovery upon illumination; approximately 80% of embryos injected with this reagent showed complete *tbxta* morphant phenotypes, as opposed to the 90% observed with the cyclic cMO.

The T-box gene, *tbx16* regulates paraxial mesoderm patterning. Zebrafish with loss-of-function *tbx16* alleles (also known as *spadetail* mutants) fail to form trunk somites, and the undifferentiated mesodermal progenitor cells accumulate in the tailbud form a spade-like structure.[51,52] In analogy to the experiments described above, we injected one-cell zebrafish zygotes with double-lariat oor cyclic *tbx16* cMOs and scored their phenotypes at 30 hpf (Figure 3B). As with the *tbxta* cMOs, the double-

lariat *tbx16* cMO exhibited less efficient functional recovery upon ultraviolet illumination than the cyclic version. To achieve light-induced phenotypes comparable to those for a 1 ng/embryo dose (115 fmol) of the cyclic *tbx16* cMO, we needed to inject 2 ng/embryo (230 fmol) of the double-lariat reagent. Nevertheless, we also observed that this higher dose of the double-lariat cMO exhibited reduced basal activity. All the embryos injected with the double-lariat reagent developed normally when cultured in the dark, but 8% of those injected with the cyclic *tbxta* cMO showed developmental defects under the same conditions. These findings demonstrate the general efficacy of double-lariat cMOs and indicate that these more conformationally constrained reagents can have lower basal activity.
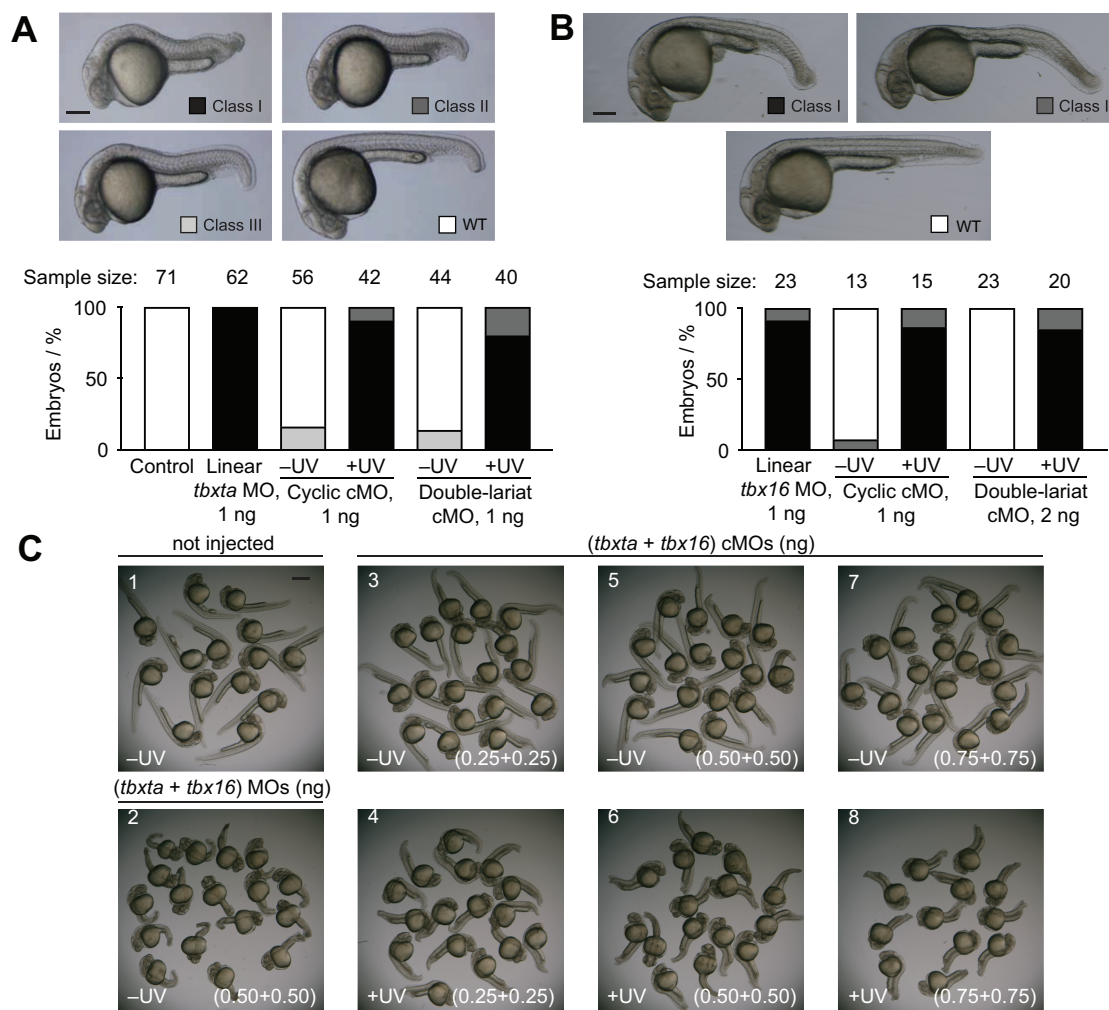

Figure 3. *In vivo* efficacy of double-lariat cMOs. Phenotypic distributions for zebrafish embryos injected with the indicated oligonucleotides and either cultured in the dark or globally irradiated with UV light at 3 - 3.5 hpf. A) Comparison of cyclic and double-lariat *tbxta* cMOs. Classification of *tbxta* loss-of-function phenotypes (I = most severe, WT = wildtype). 24-hpf embryos are shown (lateral view). Scale bar = 200 μm. B) Comparison of cyclic and double-lariat *tbx16* cMOs. Classification of *tbx16* loss-of-function phenotypes (I = most severe, WT = wildtype). 30-hpf embryos are shown. Scale bar = 200 μm. C) Co-injection of *tbxta* and *tbx16* linear MOs (2) and double-lariat cMOs (3-8). Double-lariat cMO-injected embryos cultured in the dark dark (3, 5, and 7) developed normally with minimal defects at higher dosage. Scale bar: 500 μm.

To conclude our studies, we sought to explore the feasibility of using double-lariat cMOs to simultaneously inactivate two genes. Our *tbxta*- and *tbx16*-targeting reagents are ideal for assessing combinatorial applications since the two T-box transcription factors have distinct roles during

mesoderm differentiation (notochord vs. somite development).[53] We injected one-cell zebrafish zygotes with varying amounts of the double-lariat *tbxta* and *tbx16* cMOs and then either globally irradiated the embryos at 3.5 hpf with ultraviolet light for 15 seconds or maintained the embryos in the dark. Most of the resulting embryos developed normally in the dark without appreciable developmental defects at 24 hpf when each double-lariat cMO was injected at up to a 0.75 ng/embryo dose. This markedly contrasts the mesoderm defects we previously observed when cyclic *tbxta* and *tbx16* cMOs were co-injected into zebrafish embryos.[35] Moreover, the double-lariat cMO-injected zebrafish (0.75 ng/embryo dose) exhibited substantial notochord and somite deficits upon exposure to ultraviolet light, albeit with less severity that that obtained with linear *tbxta* and *tbx16* MOs. Taken together, our studies establish that double-lariat cMOs are valuable reagents for optical gene silencing, with reduced basal activity but also lower functional recovery in comparison to cyclic cMOs.

CONCLUSION

In summary, we have designed and synthesized cMOs with a double-lariat structure, utilizing a self-immolative linker that releases three components with a single photolysis event. With its smaller macrocycles, the double-lariat cMOs can exhibit lower dark-state activity than their cyclic counterparts, thereby validating the concept that increased MO curvature is associated with reduced RNA binding. Finally, the best of our knowledge, this is the first example of a short oligonucleotide (~25 bases) with a double-lariat or bicyclic oligonucleotide geometry. While short bicyclic peptides have been shown to have better drug-like properties and improved cell-penetration capabilities,[40,54] with the exception of few longer bi/multicyclic geometries (36 bases[55] and 90 bases[56]), analogous bicyclic oligonucleotides have not been reported in the literature.

Taking advantage of this diminished 'leakiness,' we could use double-lariat cMOs targeting *tbxta* or *tbx16* in combination to achieve light-dependent defects in both axial and paraxial mesoderm derivatives. The extent to which this basal activity is reduced varied between the *tbxta*- and *tbx16*-targeting reagents, and we surmise that this reflects differences in the secondary and tertiary structures or binding proteins of the targeted mRNAs. We also noted that the double-lariat cMOs do not fully reach the uncaging level of cyclic cMOs. This is possibly due to non-quantitative linearization of the caged structure after linker photolysis, which could result from incomplete 1,6-elimination. In addition, the internal aminophenyltriazole scar in the photoreleased MO might reduce mRNA hybridization efficiency. As with the varying basal activities of the double-lariat cMOs, this effect appears to be target-dependent since functional recovery of the photolyzed *tbx16* cMO was more reduced than that of *tbxta*-targeting reagent. Our findings therefore suggest ways in which cMOs could be further improved. For example, basal activities can be further diminished by tethering the MO termini to an internal nucleobase rather than phosphorodiamidate linkage, impeding RNA hybridization by both conformational constraints and loss of Watson-Crick base-pairing. Alternative

self-immolative linkers with more rapid elimination kinetics or scarless photorelease chemistry could also improve the functional recovery of double-lariat cMOs after photolysis.

We anticipate that further development of double-lariat cMOs will lead to versatile reagents for controlling multiple genes in whole organisms. These conformationally constrained oligonucleotides could not only enable the study of complex genetic networks that regulate tissue formation but might also find applications in oligonucleotide-based drug design.

ASSOCIATED CONTENT

Supporting Information containing supplementary figures, synthetic procedures, NMR data, and mass spectra.

REFERENCES

(1) Forlani, G.; Di Ventura, B. Light express. *Curr. Opin. Syst. Biol.* **2021**, *28*, 100356.

(2) Ankenbruck, N.; Courtney, T.; Naro, Y.; Deiters, A. Optochemical Control of Biological Processes in Cells and Animals. *Angew Chem Int. Ed.* **2018**, *57* (11), 2768-2798.

(3) Hartmann, D.; Smith, J. M.; Mazzotti, G.; Chowdhry, R.; Booth, M. J. Controlling gene expression with light: a multidisciplinary endeavour. *Biochem. Soc. Trans.* **2020**, *48* (4), 1645-1659.

(4) Hughes, R. M. A compendium of chemical and genetic approaches to light-regulated gene transcription. *Crit. Rev. Biochem. Mol. Biol.* **2018**, *53* (5), 453-474.

(5) Shestopalov, I. A.; Chen, J. K. Oligonucleotide-based tools for studying zebrafish development. *Zebrafish* **2010**, *7* (1), 31-40.

(6) Bardhan, A.; Deiters, A.; Ettensohn, C. A. Conditional gene knockdowns in sea urchins using caged morpholinos. *Dev. Biol.* **2021**, *475*, 21-29.

(7) Hozumi, A.; Horie, T.; Sasakura, Y. Neuronal map reveals the highly regionalized pattern of the juvenile central nervous system of the ascidian Ciona intestinalis. *Dev. Dyn.* **2015**, *244* (11), 1375-1393.

(8) Darrah, K. E.; Deiters, A. Translational control of gene function through optically regulated nucleic acids. *Chem. Soc. Rev.* **2021**, *50* (23), 13253-13267.

(9) Housden, B. E.; Muhar, M.; Gemberling, M.; Gersbach, C. A.; Stainier, D. Y.; Seydoux, G.; Mohr, S. E.; Zuber, J.; Perrimon, N. Loss-of-function genetic tools for animal models: cross-species and cross-platform differences. *Nat. Rev. Genetics* **2017**, *18* (1), 24-40.

(10) Corey, D. R.; Abrams, J. M. Morpholino antisense oligonucleotides: tools for investigating vertebrate development. *Genome Biol* **2001**, *2* (5), Reviews1015.

(11) Blum, M.; De Robertis, E. M.; Wallingford, J. B.; Niehrs, C. Morpholinos: Antisense and Sensibility. *Dev. Cell.* **2015**, *35* (2), 145-149.

(12) Moulton, H. M., Mounton, J. D. Edited Morpholino Oligomers Methods and Protocols; *Methods Mol. Biol.* Humana Press, Springer, 2017.

(13) Summerton, J.; Weller, D. Morpholino antisense oligomers: design, preparation, and properties. *Antisense Nucleic Acid Drug Dev.* **1997**, *7* (3), 187-195.

(14) Shadid, M.; Badawi, M.; Abulrob, A. Antisense oligonucleotides: absorption, distribution, metabolism, and excretion. *Expert Opin. Drug Metab. Toxicol.* **2021**, *17* (11), 1281-1292.

(15) Ekker, S. C.; Larson, J. D. Morphant technology in model developmental systems. *Genesis* **2001**, *30* (3), 89-93.

(16) Shestopalov, I. A.; Chen, J. K. Chemical technologies for probing embryonic development. *Chem. Soc. Rev.* **2008**, *37* (7), 1294-1307.

(17) Shestopalov, I. A.; Sinha, S.; Chen, J. K. Light-controlled gene silencing in zebrafish embryos. *Nat. Chem. Biol.* **2007**, *3* (10), 650-651.

(18) Ouyang, X.; Shestopalov, I. A.; Sinha, S.; Zheng, G.; Pitt, C. L.; Li, W. H.; Olson, A. J.; Chen, J. K. Versatile synthesis and rational design of caged morpholinos. *J. Am. Chem. Soc.* **2009**, *131* (37), 13255-13269.

(19) Tallafuss, A.; Gibson, D.; Morcos, P.; Li, Y.; Seredick, S.; Eisen, J.; Washbourne, P. Turning gene function ON and OFF using sense and antisense photo-morpholinos in zebrafish. *Development* **2012**, *139* (9), 1691-1699.

(20) Tomasini, A. J.; Schuler, A. D.; Zebala, J. A.; Mayer, A. N. PhotoMorphs: a novel light-activated reagent for controlling gene expression in zebrafish. *Genesis* **2009**, *47* (11), 736-743.

(21) Deiters, A.; Garner, R. A.; Lusic, H.; Govan, J. M.; Dush, M.; Nascone-Yoder, N. M.; Yoder, J. A. Photocaged morpholino oligomers for the light-regulation of gene function in zebrafish and Xenopus embryos. *J. Am. Chem. Soc.* **2010**, *132* (44), 15644-15650.

(22) Liu, Q.; Deiters, A. Optochemical control of deoxyoligonucleotide function via a nucleobase-caging approach. *Acc. Chem. Res.* **2014**, *47* (1), 45-55.

(23) Yamazoe, S.; Shestopalov, I. A.; Provost, E.; Leach, S. D.; Chen, J. K. Cyclic caged morpholinos: conformationally gated probes of embryonic gene function. *Angew. Chem. Int. Ed.* **2012**, *51* (28), 6908-6911.

(24) Wang, Y.; Wu, L.; Wang, P.; Lv, C.; Yang, Z.; Tang, X. Manipulation of gene expression in zebrafish using caged circular morpholino oligomers. *Nucleic Acids Res.* **2012**, *40* (21), 11155-11162.

(25) Ramstein, J.; Lavery, R. Energetic coupling between DNA bending and base pair opening. *Proc. Natl. Acad. Sci. U. S. A.* **1988**, *85* (19), 7231-7235.

(26) Yamazoe, S.; Liu, Q.; McQuade, L. E.; Deiters, A.; Chen, J. K. Sequential gene silencing using wavelength-selective caged morpholino oligonucleotides. *Angew. Chem. Int. Ed.* **2014**, *53* (38), 10114-10118.

(27) Pattanayak, S.; Vázquez-Maldonado, L. A.; Deiters, A.; Chen, J. K. Combinatorial control of gene function with wavelength-selective caged morpholinos. *Methods Enzymol.* **2019**, *624*, 69-88.

(28) Yamazoe, S.; McQuade, L. E.; Chen, J. K. Nitroreductase-activatable morpholino oligonucleotides for in vivo gene silencing. *ACS Chem. Biol.* **2014**, *9* (9), 1985-1990.

(29) Darrah, K.; Wesalo, J.; Lukasak, B.; Tsang, M.; Chen, J. K.; Deiters, A. Small Molecule Control of Morpholino Antisense Oligonucleotide Function through Staudinger Reduction. *J. Am. Chem. Soc.* **2021**, *143* (44), 18665-18671.

(30) Griepenburg, J. C.; Rapp, T. L.; Carroll, P. J.; Eberwine, J.; Dmochowski, I. J. Ruthenium-Caged Antisense Morpholinos for Regulating Gene Expression in Zebrafish Embryos. *Chem. Sci.* **2015**, *6* (4), 2342-2346.

(31) Deodato, D.; Dore, T. M. Practical Synthesis of Quinoline-Protected Morpholino Oligomers for Light-Triggered Regulation of Gene Function. *Molecules* **2020**, *25* (9).

(32) Gutzman, J. H.; Graeden, E.; Brachmann, I.; Yamazoe, S.; Chen, J. K.; Sive, H. Basal constriction during midbrain-hindbrain boundary morphogenesis is mediated by Wnt5b and focal adhesion kinase. *Biol. Open* **2018**, *7* (11).

(33) Shestopalov, I. A.; Pitt, C. L.; Chen, J. K. Spatiotemporal resolution of the Ntla transcriptome in axial mesoderm development. *Nat. Chem. Biol.* **2012**, *8* (3), 270-276.

(34) Payumo, A. Y.; McQuade, L. E.; Walker, W. J.; Yamazoe, S.; Chen, J. K. Tbx16 regulates hox gene activation in mesodermal progenitor cells. *Nat. Chem. Biol.* **2016**, *12* (9), 694-701.

(35) Payumo, A. Y.; Walker, W. J.; McQuade, L. E.; Yamazoe, S.; Chen, J. K. Optochemical dissection of T-box gene-dependent medial floor plate development. *ACS Chem. Biol.* **2015**, *10* (6), 1466-1475.

(36) Carl, P. L.; Chakravarty, P. K.; Katzenellenbogen, J. A. A novel connector linkage applicable in prodrug design. *J. Med. Chem.* **1981**, *24* (5), 479-480.

(37) Alouane, A.; Labruère, R.; Le Saux, T.; Schmidt, F.; Jullien, L. Self-immolative spacers: kinetic aspects, structure-property relationships, and applications. *Angew. Chem. Int. Ed.* **2015**, *54* (26), 7492-7509.

(38) Weller, D. D.; Hassinger, J. N.; Cai, B. Z. Oligonucleotide analogs having cationic intersubunit linkages. *US Patent* US7943762B2, 2011.

(39) Mellbye, B. L.; Weller, D. D.; Hassinger, J. N.; Reeves, M. D.; Lovejoy, C. E.; Iversen, P. L.; Geller, B. L. Cationic phosphorodiamidate morpholino oligomers efficiently prevent growth of Escherichia coli in vitro and in vivo. *J. Antimicrob. Chemother.* **2010**, *65* (1), 98-106.

(40) Davies, S.; Oliveira, B. L.; Bernardes, G. J. L. Development of a self-immolative linker for tetrazine-triggered release of alcohols in cells. *Org. Biomol. Chem.* **2019**, *17* (23), 5725-5730.

(41) Shahsavari, S.; Gooding, J.; Wigstrom, T.; Fang, S. Formation of Hindered Arylcarbamates using Alkyl Aryl Carbonates under Highly Reactive Conditions. *ChemistrySelect* **2017**, *2* (13), 3959-3963.

(42) Saha, A. K.; Rapoport, H.; Schultz, P. 1, 1'-Carbonylbis (3-methylimidazolium) triflate: an efficient reagent for aminoacylations. *J. Am. Chem. Soc.* **1989**, *111* (13), 4856-4859.

(43) Pattanayak, S.; Paul, S.; Nandi, B.; Sinha, S. Improved protocol for the synthesis of flexibly protected morpholino monomers from unprotected ribonucleosides. *Nucleos. Nucleot. Nucleic Acids* **2012**, *31* (11), 763-782.

(44) Bhadra, J.; Pattanayak, S.; Sinha, S. Synthesis of Morpholino Monomers, Chlorophosphoramidate Monomers, and Solid-Phase Synthesis of Short Morpholino Oligomers. *Curr. Protoc. Nucleic Acid Chem.* **2015**, *62*, 4.65.61-26.

(45) Pattanayak, S.; Sinha, S. Lithium bromide–DBU mediated synthesis of chlorophosphoramidate-activated morpholino nucleoside subunits. *Tetrahedron Lett.* **2012**, *53* (49), 6714-6717.

(46) Giustarini, D.; Dalle-Donne, I.; Colombo, R.; Milzani, A.; Rossi, R. Is ascorbate able to reduce disulfide bridges? A cautionary note. *Nitric Oxide* **2008**, *19* (3), 252-258.

(47) Li, X.; Gartner, Z. J.; Tse, B. N.; Liu, D. R. Translation of DNA into synthetic N-acyloxazolidines. *J. Am. Chem. Soc.* **2004**, *126* (16), 5090-5092.

(48) Schulte-Merker, S.; van Eeden, F. J.; Halpern, M. E.; Kimmel, C. B.; Nüsslein-Volhard, C. no tail (ntl) is the zebrafish homologue of the mouse T (Brachyury) gene. *Development* **1994**, *120* (4), 1009-1015.

(49) Halpern, M. E.; Ho, R. K.; Walker, C.; Kimmel, C. B. Induction of muscle pioneers and floor plate is distinguished by the zebrafish no tail mutation. *Cell* **1993**, *75* (1), 99-111.

(50) Showell, C.; Binder, O.; Conlon, F. L. T-box genes in early embryogenesis. *Dev. Dyn.* **2004**, *229* (1), 201-218.

(51) Kimmel, C. B.; Kane, D. A.; Walker, C.; Warga, R. M.; Rothman, M. B. A mutation that changes cell movement and cell fate in the zebrafish embryo. *Nature* **1989**, *337* (6205), 358-362.

(52) Griffin, K. J.; Amacher, S. L.; Kimmel, C. B.; Kimelman, D. Molecular identification of spadetail: regulation of zebrafish trunk and tail mesoderm formation by T-box genes. *Development* **1998**, *125* (17), 3379-3388.

(53) Amacher, S. L.; Draper, B. W.; Summers, B. R.; Kimmel, C. B. The zebrafish T-box genes no tail and spadetail are required for development of trunk and tail mesoderm and medial floor plate. *Development* **2002**, *129* (14), 3311-3323.

(54) Lian, W.; Jiang, B.; Qian, Z.; Pei, D. Cell-permeable bicyclic peptide inhibitors against intracellular proteins. *J. Am. Chem. Soc.* **2014**, *136* (28), 9830-9833.

(55) Chaudhuri, N. C.; Kool, E. T. Very High Affinity DNA Recognition by Bicyclic and Cross-Linked Oligonucleotides. *J. Am. Chem. Soc.* **1995**, *117* (42), 10434-10442.

(56) Seyfried, P.; Eiden, L.; Grebenovsky, N.; Mayer, G.; Heckel, A. Photo-Tethers for the (Multi-)Cyclic, Conformational Caging of Long Oligonucleotides. *Angew Chem Int. Ed.* **2017**, *56* (1), 359-363.